Effect of radiative cooling on the size-dependent stability of small boron clusters

Piero Ferrari,[1] Jan Vanbuel,[1] Klavs Hansen,[1,2] Peter Lievens,[1] Ewald Janssens,[1,*] and André Fielicke[3]

[1]*Laboratory of Solid State Physics and Magnetism, KU Leuven, 3001 Leuven, Belgium*

[2]*Center for Joint Quantum Studies and Department of Physics, Tianjin University, Tianjin 300072, China and Department of Physics, Gothenburg University, 41296 Gothenburg, Sweden*

[3]*Fritz-Haber-Institut der Max-Planck-Gesellschaft, 14195 Berlin, Germany*

(Received 4 May 2018; published 2 July 2018)

The mass spectrum of cationic boron clusters, B_N^+ ($N = 5 - 20$), after photoexcitation demonstrates that radiative cooling is an important, though often neglected, process in determining the relative stability of small and isolated particles. The observed intensities in mass spectra suggest that B_5^+, B_{11}^+, B_{13}^+, and B_{15}^+ are particularly stable clusters, consistent with density-functional theory calculations. Quantitative agreement, however, is only obtained if radiative cooling is included in the analysis. All clusters are found to radiate on microsecond timescales, suggesting recurrent fluorescence as the dominant photon emission process.

DOI: 10.1103/PhysRevA.98.012501

I. INTRODUCTION

The reduction of matter to the nanoscale leads to the emergence of a wide range of new physical phenomena. In clusters, systems composed of a countable number of atoms, quantum confinement effects appear prominently and properties become highly size dependent [1]. Stability is one of the more important properties of clusters, because highly stable clusters are most likely to retain their integrity when deposited on surfaces, which is of prime importance for applications in both optics and catalysis [2,3].

The stability of small gas-phase clusters is conveniently studied by photofragmentation, a technique in which clusters are exposed to an intense laser beam, and the products are analyzed by mass spectrometry [4]. These types of experiments are often analyzed disregarding any cooling channel other than fragmentation. Recent experiments, however, have shown that small carbon and metal clusters can cool radiatively [5–11], in some cases at very high rates.

In this work we show that radiative cooling is crucial when analyzing size-to-size stabilities by investigating small cationic boron clusters. The structures of boron clusters are extensively studied because of their remarkable bonding mechanism, resulting from their electron deficient nature and the interplay between electron localization and delocalization [12–15]. Boron clusters have unusual structures, adopting planar or quasiplanar configurations below $N = 16$, whereas larger clusters are predicted to adopt cylindrical structures [14,16]. B_{40} has been proposed to adopt a fullerenelike cage configuration [15]. The stability patterns of boron clusters have also been investigated [17]. Collision induced dissociation experiments suggest B_{13}^+ to be a particularly stable cluster, due to a unique type of triple-aromatic bonding [18,19]. Fluxionality has also been observed in B_{13}^+ [16], suggesting its use in novel applications, for example, as a molecular Wankel engine [20].

II. EXPERIMENTAL METHODS

Understanding the cooling processes and demonstrating their relevance for the size-dependent cluster stabilization are achieved in this work by studying photofragmentation of isolated clusters using mass spectrometry. Boron clusters are produced by laser ablation of an isotopically enriched ^{11}B rod [21,16]. The ablated plasma is cooled by a pulse of He gas that triggers cluster formation. The cluster beam expands into vacuum and is collimated by a 1-mm-diameter skimmer before entering a reflectron time-of-flight (TOF) mass spectrometer. Charged species produced in the source are deflected from the molecular beam by applying a constant voltage of 30 V to the first grid of the extraction stage of the mass spectrometer. The remaining neutral clusters are excited by a tightly focused pulsed F_2 laser (1 mJ, 157 nm). Nonresonant multiphoton absorption induces ionization and fragmentation, after which the products are analyzed by mass spectrometry.

III. RESULTS

A mass spectrum recorded after photofragmentation of initially neutral clusters is presented in Fig. 1, and shows strong size-to-size intensity variations. B_5^+, B_{11}^+, B_{13}^+, and B_{15}^+ are found with relatively enhanced abundances, while $N =$ 6, 12, 14, and 16 are local abundance minima, and strong odd-even intensity oscillations are seen for $N > 10$. These size-dependent intensity variations are in agreement with a previous study in which the cluster fragmentation was induced by collisions [17]. As a first description of stability, B_5^+, B_{11}^+, B_{13}^+, and B_{15}^+ are suggested to have a higher dissociation energy (D_N) and thus to be more stable than their precursors in the fragmentation chain induced by photon absorption.

The fragmentation channels of the clusters can be identified by TOF mass spectrometry. Following multiphoton absorption, fragmentation can take place on submicrosecond timescales, which is much faster than the timescale of the experiment. Hence, the corresponding fragments are called prompt fragments. However, clusters with a lower excitation energy may

*Corresponding author: ewald.janssens@kuleuven.be

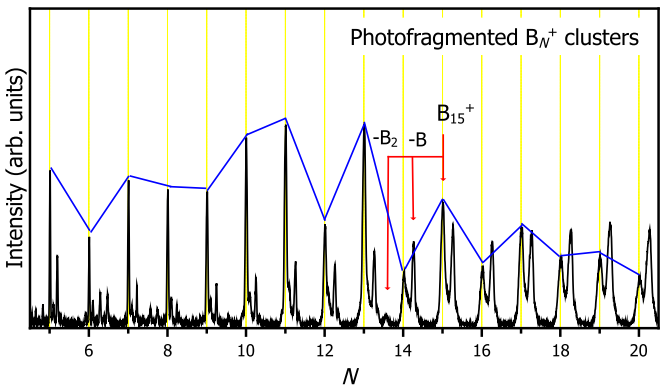

FIG. 1. Distribution of B_N^+ clusters produced by photofragmentation of neutral species using a focused VUV laser (157 nm). The blue lines are used to visualize the intensity patterns of prompt (quasi-instantaneous) fragments. The prompt B_{15}^+ cluster is marked in the figure, together with its metastable fragments B_{14}^+ and B_{13}^+ produced by monomer and dimer evaporation, respectively.

fragment at longer timescales in a metastable fragmentation process. If this process occurs during the free flight between the extraction and reflection stages of the mass spectrometer, the products show up as additional peaks in the mass spectrum. Such peaks are clearly visible in Fig. 1, next to each prompt fragment. The identity of the fragments is determined by their flight time with simple electrostatics [6]. An example of the fragment peak assignment is presented in Fig. 1 for the metastable monomer and dimer evaporation of the prompt B_{15}^+ cluster. Metastable decay is observed for all clusters in this study, and is quantified as the relative amount of metastable decay, M_N, whether a monomer or a dimer loss (fractions are defined as the intensity of the metastable peaks in mass spectra normalized by the total intensity of prompt plus monomer and dimer metastable fragmentation peaks). These fractions are given in Fig. 2, showing that monomer evaporation is the preferred dissociation channel for most sizes. Dimer evaporation is a competing channel for B_9^+, B_{11}^+, and B_{15}^+ only. Density-functional theory (DFT) calculations (see Ref. [22]) predicted a lower D_N for monomer evaporation than for dimer loss, which tends to favor the monomer evaporation

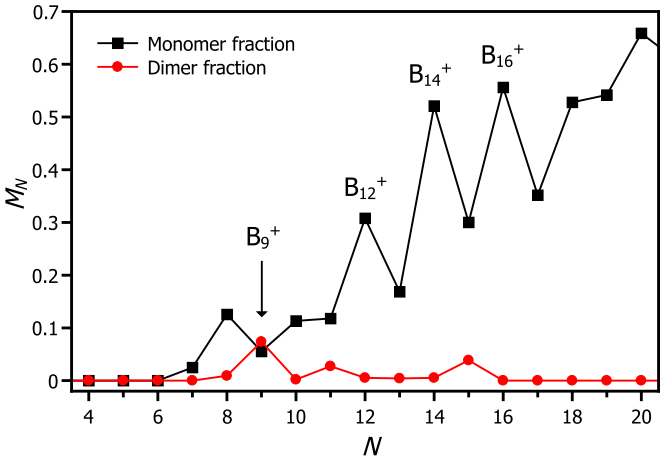

FIG. 2. Monomer (black squares) and dimer (red circles) metastable fractions, extracted from the mass spectrum of Fig. 1.

channel, in line with the experiments. A second observation from Fig. 2 is that, besides size-to-size variations, the overall metastable fractions increase with cluster size. This is a well-understood phenomenon, related to the clusters' heat capacity [23].

Radiative cooling rates of B_N^+ ($N = 8 - 20$) clusters can be inferred using variable ion extraction times, previously applied in the investigation of laser heated fullerenes [24], niobium [7], silicon [6], and gold [8] clusters. The method is based on the fact that, in the absence of radiation, clusters excited in a broad distribution of energies have fragmentation rates that follow a $1/t$ dependence in time, with $t = 0$ the moment of excitation. This situation is realized under the non-resonant multiphoton absorption conditions here. Thus, in the absence of radiation, the amount of metastable fragmentation is proportional to $\ln(t_2/t_1)$, where t_1 represents the time elapsed from the moment of laser excitation until mass selection at extraction, and t_2 the time from laser excitation until entry into the reflectron stage of the mass spectrometer. Deviation from this dependence signals the presence of a competing and unobserved decay process. Only radiative cooling qualifies as a candidate for this channel in this case.

The fragmentation decay rate in the presence of radiative cooling can be expressed as in Eq. (1),

$$R_N(t) \propto \frac{e^{-k_{p,N}t}}{t}, \tag{1}$$

where $k_{p,N}$ represents the rate of photon emission. In the limit that radiative cooling is absent, i.e., $k_{p,N} = 0$, the $1/t$ decay law for fragmentation is recovered. Integration of Eq. (1) between t_1 and t_2 gives the amount of metastable fragmentation,

$$M_N = a_N \int_{t_1}^{t_2} \frac{e^{-k_{p,N}t}}{t} dt, \tag{2}$$

with a_N a proportionality constant. To determine $k_{p,N}$ experimentally, ion extraction at the mass spectrometer is delayed with respect to laser excitation by a small amount Δt. This changes the flight times to $t_{1,2} = t_{1,2}^{(0)} + \Delta t$ and Eq. (2) is fitted with $k_{p,N}$ and a_N as free parameters. $t_1^{(0)}$ and $t_2^{(0)}$ are given by the motion through the fields and field-free regions [6]. These are $t_1^{(0)} = (0.043 + 0.118\sqrt{N})\ \mu$s and $t_2^{(0)} = (0.06 + 5.74\sqrt{N})\ \mu$s. The presence of radiative cooling can be identified by applying a leading-order Taylor expansion to Eq. (2), which gives Eq. (3) under the condition $k_{p,N}t < 1$. For the analysis, Eq. (2) is used without any approximation.

$$M_N = a_N \ln\left(\frac{t_2}{t_1}\right) - k_{p,N} a_N (t_2 - t_1). \tag{3}$$

Thus, to this order, a plot of M_N versus $\ln(t_2/t_1)$ should give a straight line intercepting the origin if clusters cool by fragmentation only, while the presence of radiative cooling results in a negative intercept. Such a plot is presented in Fig. 3(a) for three boron clusters: B_9^+, B_{14}^+, and B_{17}^+. This analysis shows that radiative cooling is present for the three studied clusters to different degrees.

The photon emission rates, obtained by fitting Eq. (2) to M_N versus Δt, are presented in Fig. 3(b). All the studied boron clusters radiate on the timescale of the experiment and the magnitude of the photon emission rate is strongly size

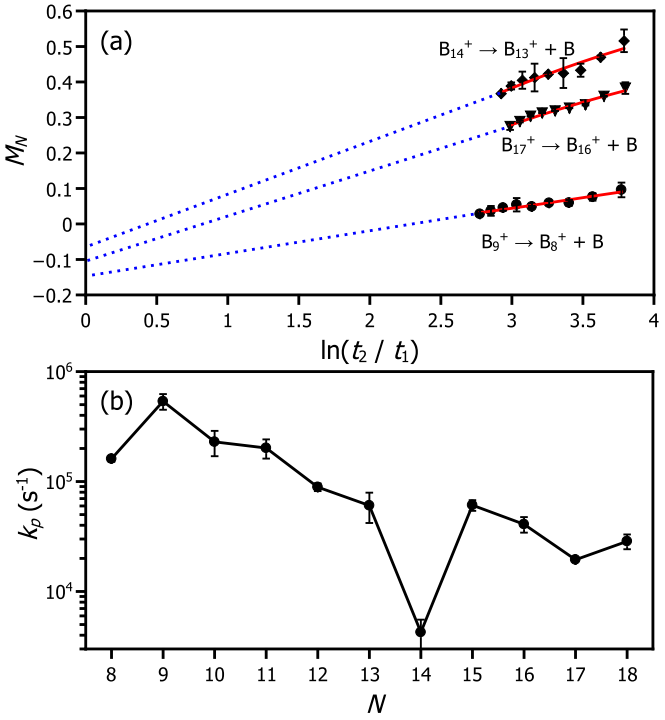

FIG. 3. (a) The metastable fraction M_N versus $\ln(t_2/t_1)$ for three boron clusters: B_9^+, B_{14}^+, and B_{17}^+. The negative intercept with the ordinate axis shows the presence of radiative cooling. (b) Rates of photon emission of B_N^+ clusters, extracted by fitting Eq. (2) to measured M_N versus Δt curves.

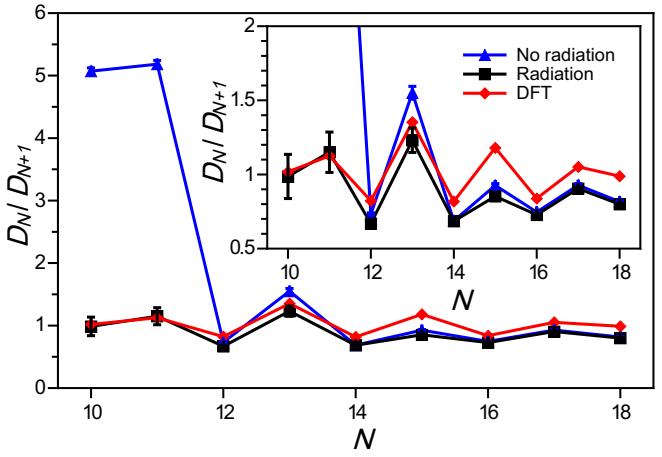

FIG. 4. Ratio of dissociation energies extracted from the metastable fractions after photofragmentation. The analysis with and without radiative cooling is presented, together with the values calculated in Ref. [22]. The inset shows a close-up of the figure. Error bars include propagation from the fitting errors of k_p and assuming a 5% uncertainty on the determination of flight times t_1 and t_2, and a similar value for the frequency factor ω.

dependent. For example, B_9^+ is found to radiate at a very high rate of $\sim 5.4 \times 10^5\ s^{-1}$, corresponding to a cooling time τ_N of 1.85 μs ($\tau_N = k_{p,N}^{-1}$). For B_{14}^+, a rate of $\sim 4.3 \times 10^3\ s^{-1}$ or a cooling time of 232 μs is obtained. There are two important conclusions about the extracted photon emission rates. First, the very high photon emission rates strongly suggest that decay proceeds via the recurrent fluorescence process, through a thermally populated electronic excited state [8,11]. This process requires the presence of electronically excited states with sufficient oscillator strength and in an appropriate energy window. To date, studies on excited states of boron clusters are scarce [25,26].

The second conclusion is that intensities in mass spectra alone are insufficient to deduce the stability patterns of the clusters, since radiative cooling is present [27]. This conclusion holds independently of the excitation process that is used to induce fragmentation of the boron clusters [17].

IV. DISCUSSION

Using the metastable fractions and the rates of photon emission, ratios of dissociation energies D_N/D_{N+1} can be extracted. The analysis, explained in detail in Refs. [23,28], is based on Eq. (4), which requires knowledge of the metastable fractions M_N and the flight times t_1 and t_2.

$$\frac{D_N}{D_{N+1}} = \frac{M_N\left[\frac{C_N}{G(t_1)} - \frac{1}{2}\right]}{M_N\left[\frac{C_N}{G(t_1)} + \frac{1}{2}\right] - \frac{C_N \ln(t_2/t_1)}{G(t_1)G(t_2)}}. \quad (4)$$

Here C_N is the heat capacity and $G(t) = \ln(\omega t)$, with ω the frequency factor in the approximate Arrhenius expression for fragmentation [23]. In the absence of radiation, t_1 and t_2 in Eq. (4) are the physical values. With these nonradiative values, the calculated dissociation energies will be in error, the more so if the radiation constant approaches t_1 ($\sim$0.5 μs). This is seen in Fig. 4 for the ratios of the sizes $N = 11$ and $N = 10$, which also have the highest radiative rate in the studied size range [the 9-mer has a branching to dimer evaporation and is not covered by Eq. (4)]. In order to include the radiative effects on the metastable fraction and hence in Eq. (4), the effective times for the termination of the decay need to be modified from the nonradiative t_1 and t_2 to shorter values, as expressed in Eq. (5) [28]. In simpler terms, the quenching effect of the photon emission effectively shortens the flight times during which metastable fragmentation can occur.

$$t' = \frac{1 - e^{-k_p t}}{k_p}. \quad (5)$$

Thus, using the experimental data of Fig. 2 relative dissociation energies can be estimated both with and without taking into account the effect of radiation. Figure 4 presents this analysis, by plotting the ratios D_N/D_{N+1} as a function of N. For both the radiative and nonradiative cases, an odd-even oscillation for the D_N/D_{N+1} ratios is found, with local maxima for odd-atom clusters. This resembles the pattern present in I_N (Fig. 1). Importantly, a remarkably improved agreement with the dissociation energies predicted by DFT calculations is found when radiative cooling is accounted. The D_N/D_{N+1} ratios obtained by DFT in Ref. [22] are included in Fig. 4. The radiative effects are particularly relevant for the smaller clusters, with their higher photon emission rates [Fig. 3(b)]. The comparison emphasizes that (i) a correct determination of relative stabilities of the clusters is only achieved when radiative cooling is included as a competing channel to fragmentation, and (ii),

there are pronounced size-to-size variations in the relative stability of the B_N^+ ($N = 10 - 17$) clusters, with odd-atom clusters having a locally higher stability. A final observation is the lower ratios extracted from the data for the larger clusters ($N = 14 - 18$), when compared to those computed by DFT. This small discrepancy can have several reasons, such as the DFT calculations itself or that abundances tend to decrease with size, affecting the calculated ratios [23]. We prefer not to speculate on the precise reasons for this phenomenon. Nevertheless, noteworthy is that the main observation of this work is not affected by this discrepancy, which is the strong effect radiative cooling has in the quantification of relative stabilities from mass spectrometric experiments.

V. CONCLUSIONS

In this work, the emission of radiation as a competing cooling channel was studied in the size range $N = 8 - 18$. Remarkably, all boron clusters are found to radiate within the timescale of the experiment, albeit with strongly varying rates. The very high rates strongly indicate recurrent fluorescence as the photon emission mechanism. Combining the information of mass spectra intensities, radiative cooling rates, and fragmentation channels, the stability patterns of the clusters were quantified by the ratios D_N/D_{N+1}. This analysis indicates a pronounced odd-even oscillation in the stability of the clusters in the $N = 10$–18 size range, with odd-atom cationic clusters being more stable. Importantly, a significantly improved agreement between experiment and theory is obtained if radiation is taken into account.

ACKNOWLEDGMENTS

This work has been supported by the Research Foundation-Flanders (FWO) and the KU Leuven Research Council (GOA/14/007). P.F. and J.V. acknowledge the FWO for financial support. A.F. thanks the Deutsche Forschungsgemeinschaft for a Heisenberg grant (No. FI 893/5).

[1] H. Häkkinen, Adv. Phys. X **1**, 467 (2016).
[2] E. N. Esenturk, J. Fettinger, Y.-F. Lam, and B. Eichhorn, Angew. Chem., Int. Ed. **116**, 2184 (2004).
[3] T. Sugai, H. Omote, S. Bandow, N. Tanaka, and H. Shinohara, J. Chem. Phys. **112**, 6000 (2000).
[4] S. Neukermans, E. Janssens, H. Tanaka, R. E. Silverans, and P. Lievens, Phys. Rev. Lett. **90**, 033401 (2003).
[5] G. Ito, T. Furukawa, H. Tanuma, J. Matsumoto, H. Shiromaru, T. Majima, M. Goto, T. Azuma, and K. Hansen, Phys. Rev. Lett. **112**, 183001 (2014).
[6] P. Ferrari, E. Janssens, P. Lievens, and K. Hansen, J. Chem. Phys. **143**, 224313 (2015).
[7] K. Hansen, Y. Li, V. Kaydashev, and E. Janssens, J. Chem. Phys. **141**, 024302 (2014).
[8] K. Hansen, P. Ferrari, E. Janssens, and P. Lievens, Phys. Rev. A **96**, 022511 (2017).
[9] S. Martin, J. Bernard, R. Brédy, B. Concina, C. Joblin, M. Ji, C. Ortega, and L. Chen, Phys. Rev. Lett. **110**, 063003 (2013).
[10] C. Breitenfeldt, K. Blaum, M. W. Froese, S. George, G. Guzmán-Ramírez, M. Lange, S. Menk, L. Schweikhard, and A. Wolf, Phys. Rev. A **94**, 033407 (2016).
[11] Y. Ebara, T. Furukawa, J. Matsumoto, H. Tanuma, T. Azuma, H. Shiromaru, and K. Hansen, Phys. Rev. Lett. **117**, 133004 (2016).
[12] A. P. Sergeeva, I. A. Popov, Z. A. Piazza, W.-L. Li, C. Romanescu, L.-S. Wang, and A. I. Boldyrev, Acc. Chem. Res. **47**, 1349 (2014).
[13] H.-J. Zhai, B. Kiran, J. Li, and L.-S. Wang, Nat. Mater. **2**, 827 (2003).
[14] E. Oger, N. R. M. Crawford, R. Kelting, P. Weis, M. M. Kappes, and R. Ahlrichs, Angew. Chem., Int. Ed. **46**, 8503 (2007).
[15] H.-J. Zhai, Y.-F. Zhao, W.-L. Li, Q. Chen, H. Bai, H.-S. Hu, Z. A. Piazza, W.-J. Tian, H.-G. Lu, Y.-B. Wu, Y.-W. Mu, G.-F. Wei, Z.-P. Liu, J. Li, S.-D. Li, and L.-S. Wang, Nat. Chem. **6**, 727 (2014).
[16] M. Fagiani, X. Song, P. Petkov, S. Debnath, S. Gewinner, W. Schöllkopf, T. Heine, A. Fielicke, and K. Asmis, Angew. Chem., Int. Ed. **56**, 501 (2017).
[17] L. Hanley, J. L. Whitten, and S. L. Anderson, J. Phys. Chem. **92**, 5803 (1988).
[18] B. Kiran, G. G. Kumar, M. T. Nguyen, A. K. Kandalam, and P. Jena, Inorg. Chem. **48**, 9965 (2009).
[19] Y. Yang, D. Jia, Y.-J. Wang, H.-J. Zhai, Y. Man, and S.-D. Li, Nanoscale **9**, 1443 (2017).
[20] J. Zhang, A. Sergeeva, M. Sparta, and A. Alexandrova, Angew. Chem., Int. Ed. **51**, 8512 (2012).
[21] C. Romanescu, D. J. Harding, A. Fielicke, and L.-S. Wang, J. Chem. Phys. **137**, 014317 (2012).
[22] T. B. Tai, N. M. Tam, and M. T. Nguyen, Theor. Chem. Acc. **131**, 1241 (2012).
[23] N. Veldeman, E. Janssens, K. Hansen, J. De Haeck, R. E. Silverans, and P. Lievens, Faraday Discuss. **138**, 147 (2008).
[24] K. Hansen and E. E. B. Campbell, J. Chem. Phys. **104**, 5012 (1996).
[25] R. He and X. C. Zeng, Chem. Commun. **51**, 3185 (2015).
[26] B. J. Nagare, S. Chavan, and V. Bambole, Comput. Theor. Chem. **1125**, 54 (2018).
[27] K. Hansen, P. Ferrari, E. Janssens, and P. Lievens, J. Phys. Chem. C **121**, 10663 (2017).
[28] K. Hansen, *Statistical Physics of Nanoparticles in the Gas Phase* (Springer, Dordrecht, 2013).